Final version published in *Journal of Physical Chemistry C*, 2017, 121 (14), pp 7985–7992.
DOI: 10.1021/acs.jpcc.7b01135

Host-guest Interaction at Molecular Interfaces: Binding of Cucurbit[7]uril on Ferrocenyl Self-assembled Monolayers on Gold

Lin Qi,[†] Huihui Tian,[†,‡] Huibo Shao,[‡,*] and Hua-Zhong Yu[†,*]

[†]*Department of Chemistry, Simon Fraser University, Burnaby, British Columbia V5A 1S6, Canada*

[‡]*College of Chemistry and Chemical Engineering, Beijing Institute of Technology, Beijing 100085, China*

ABSTRACT

Ferrocene (Fc) encapsulated cucurbit[7]uril (CB[7]) supramolecular host-guest complex (Fc@CB[7]) as a synthetic recognition pair has been widely adapted for coupling biomolecules and nanomaterials due to its ultra-high binding affinity. In this paper, we have explored the binding of CB[7] on binary ferrocenylundecanethiolate/octanethiolate self-assembled monolayer on gold (FcC11S-/C8S-Au), a model system to deepen our understanding of host-guest chemistry at molecular interfaces. It has been shown that upon incubation with CB[7] solution, the redox behavior FcC11S-/C8S-Au changes remarkably, i.e., a new pair of peaks appeared at more positive potential with narrowed widths. The ease of quantitation of surface bound-redox species (Fc^+/Fc and Fc^+@CB[7]/ Fc@CB[7]) enabled us to determine the thermodynamic formation constant of Fc@CB[7] at FcC11S-/C8S-Au ($7.3\pm1.8 \times 10^4$ M^{-1}). With time-dependent redox responses, we were able to, for the first time, deduce both the binding and dissociation rate constants, $2.8\pm0.3 \times 10^3$ $M^{-1}s^{-1}$ and 0.08 ± 0.01 s^{-1}, respectively. These results showed substantial differences both thermodynamically and kinetically for the formation of host-guest inclusion complex at molecular interfaces with respect to solution-diffused, homogenous environments.

---

* Corresponding authors; hogan_yu@sfu.ca (H.Y.); hbs@bit.edu.cn (H.S.)

1. INTRODUCTION

Different from traditional chemistry based on covalent bonding among atoms, supramolecular chemistry focuses on the self-assembly between host and guest molecules via noncovalent intermolecular interactions, which is essential for understanding many crucial biorecognition processes and has broad applications in interdisciplinary areas such as nanotechnology, enzymatic catalysis, and drug delivery.[1,2] In particular, the macrocyclic cucurbit[n]urils (CB[n]) family as a unique type of supramolecular host molecules has gained much interest in their preparation, functionalization, and application owning to their strong interactions with small guest molecules.[3-8] The synthesis of CB[6] was first reported in 1905 by condensation of glycouril and formaldehyde in concentrated HCl,[9] nearly 90 years later other CB[n] compounds (e.g., CB[5], CB[7] ~ CB[10]) were prepared by conducting the reaction under mild and kinetically controlled conditions (e.g., lower temperature) and by separating those compounds through fractional crystallization and dissolution.[10,11] Characterizations by X-ray crystallography have confirmed that CB[n] host families have a pumpkin or barrel shape with an inner hydrophobic cavity and two identical portals.[10,12] In contrast to other host molecules such as cyclodextrins (CDs), which encapsulate the guest inside their inner cavities merely through hydrophobic interactions, the electronegative carbonyl portals of CB[n] can provide additional ion-dipole interactions with positively charged cationic guests.[4] The release of high energy water molecules from the inner cavity of CB[n] is also a major driving force for forming highly stable host-guest inclusion complexes.[13]

Among CB[n] host families, CB[7] is an important member due to its higher solubility in water and strong binding affinity with certain guest molecules.[14-16] The intermediate size of CB[7] allows the incorporation of optimized number of water molecules, which releases maximum enthalpy upon their complete removal from the inner cavity to bulk solution.[13] It has been confirmed that CB[7] can form highly stable inclusion complexes with neutral ferrocene (Fc) and its cationic derivatives (as guests), which is mainly due to the perfect fit between the Fc aromatic cp rings and the CB[7] inner cavity (Scheme 1A). Their binding affinities determined by 1H NMR and ITC competition experiments are as high as $10^9 \sim 10^{15}$ M^{-1},[17] which is even stronger than the natural antigen-antibody interaction, and comparable with the biotin-avidin binding.[14] Besides the high binding affinity, the Fc@CB[7] binding pair also has the advantages of high thermo-stability, long-term durability, and unprecedented resistance to enzymatic degradation. Moreover, its binding affinity is sensitive to the environmental factors (e.g., solvent, pH, and ionic strength), which makes it possible to dissociate

without the need of harsh conditions. These advantages allow Fc@CB[7] to be applied as a substitute of natural binding pairs for immobilizing biomolecules onto molecular interfaces for different purposes.[14,18] Due to the limited modification efficiency on CB[7] (5 % ~ 10 %),[19] the general strategy is to directly deposit CB[7] on gold surface for capturing Fc-labelled targets.[20-23] However, the binding affinity for the inclusion complex formed between Fc-labelled peptides and CB[7] assembled on gold surface was found to be limitted,[24] which raises the question about the stability of Fc@CB[7] formed at molecular interfaces.

Previous electrochemical and morphological characterizations have confirmed that the structure of physically deposited CB[7] monolayer on gold is far from perfect,[25,26] which may cause strong steric hindrance for the interaction between Fc and CB[7]. Another concern is the relatively weak gold-carbonyl interaction,[27] as a result CB[7] may be easily removed from gold surface. In order to investigate the nature of Fc@CB[7] host-guest interaction at molecular interfaces, and to explore alternative routes to the application of Fc@CB[7] host-guest interaction for biochip/biosensor fabrication, herein we propose to adapt "near ideal" binary ferrocenylalkanethiolate/n-alkanethiolate SAMs on gold to investigate the host-guest interaction between CB[7] in bulk solution and Fc tethered on surface. Due to the strong gold-sulfur interaction and the hydrophobic interaction among alky chains, the binary SAMs are closely-packed and highly oriented on gold surface.[28-30] The Fc terminal groups as the binding sites for CB[7] can be well-isolated with the molar ratio of ferrocenylalkanthiols kept below 10 % during the coadsorption with n-alkanethiols.[31,32] These structural properties of the binary ferrocenylalkanethiolate/alkanethiolate SAMs can simplify the environmental factors for us to investigate the interaction between CB[7] and Fc at molecular interfaces. The other essential aspect of these highly organized molecular systems is the strong and reversible redox responses of the surface tethered Fc,[31-34] which can be conveniently employed to quantitate the Fc@CB[7] host-guest interactions via conventional electrochemical measurements (e.g., cyclic voltammetry).

2. EXPERIMENTAL SECTION

2.1. Reagents and Materials

11-Ferrocenyl-1-undecanethiol (98 %) was purchased from Dojindo Laboratories Inc. (Tokyo, Japan); 1-octanethiol (C8SH) and sodium perchlorate ($NaClO_4$) were purchased from Sigma Aldrich (St. Louis, United States). Ethanol (95 %) was from Commercial Alcohols (Toronto, Canada). All chemicals were of ACS reagent-grade and used as received. Gold slides (regular glass slides covered

with 5 nm Cr and 100 nm Au) were purchased from Evaporated Metal Films (EMF) Inc. (New York, United States).

2.2. Preparation of binary ferrocenylundecanethiolate/octanethiolate SAMs on gold (FcC11S-/C8S-Au)

Small pieces of gold slides (1×2 cm^2) were cleaned by immersion in a *Piranha* solution (3:1 mixture of concentrated H_2SO_4 and 30% H_2O_2) for 5-7 min at 90 °C (CAUTION: *Piranha solution reacts violently with organics*, *thus it must be handled with extreme caution*). Subsequently, the cleaned gold slide was rinsed with copious amounts of deionized water; then the surface was gently blown dry under N_2.

Freshly cleaned gold slides were immersed in a binary FcC11SH/C8SH ethanol solution (95%) at room temperature for overnight (> 12 h). The total concentration of the thiols is 1.0 mM with 5 % (mole fraction) of FcC11SH. The modified gold slides were washed with copious amounts of ethanol and deionized water.

2.3. Surface characterization

Reflection-absorption Infrared spectra of FcC11S-/C8S-Au before and after immersing with 1.0 mM CB[7] for 180 min were obtained by using a Nicolet Magna 560 Fourier transform infrared spectrometer (Madison, WI) equipped with an automated VeeMAX II variable angle accessory (Pike Technologies, Madison, WI). The p-polarized IR laser was incident at 80°, and the reflected beam was measured with a mercury cadmium telluride (MCT) detector upon cooling with liquid nitrogen.

Water contact angles were measured by using a goniometer (AST VCA system, Billerica, MA) immediately after adding 1.0 μL water droplets on FcC11S-/C8S-Au before and after immersing with 1.0 mM CB[7] for 180 min.

2.4. Electrochemical Measurements

Electrochemical measurements were carried out in a three-electrode, single-chamber Teflon cell with a CHI 1040A Electrochemical Analyzer (Austin, United States). The cell was constructed with an opening at the side, where the working electrode (gold slide) was attached via an O-ring seal. The surface area of the working electrode (0.150 cm^2) was estimated based on the Randles-Sevcik equation by measuring the CVs in 1.0 mM aqueous $K_3Fe(CN)_6$ at varied scan rates.[35] A platinum wire was used as the counter-electrode, and an Ag | AgCl | 3 M NaCl electrode was used as the

reference-electrode. All the CV measurements were performed in a Faraday cage at room temperature, under the protection of Ar.

3. RESULTS AND DISCUSSION

As shown in Scheme 1A, the size of a ferrocene molecule is slightly smaller than the inner cavity of CB[7], which forms the basis of strong interaction between the two.[17] As mentioned above, detailed studies of the host-guest interaction between CB[7] and ferrocene at molecular interfaces have been limited; herein we have prepared binary ferrocenylundecanethiolate/octanethiolate SAMs on gold (FcC11S-/C8S-Au) (Scheme 1B) as a model system for this purpose. In particular, we have used a low mole fraction of FcC11SH (5 %) and a short diluent (C8SH) to ensure that Fc terminal groups are well isolated, exposed, and uniformly distributed on the surface (Scheme 1B).

The formation of Fc@CB[7] on FcC11S-/C8S-Au was first confirmed by IR spectroscopy (Figure 1). The IR spectra in the C-H stretching region for FcC11S-/C8S-Au before and after incubation with CB[7] both showed typical CH_2 and CH_3 bands, and the CH band of Fc cp ring (at 3104 cm^{-1}).[36,37] While there are no changes in the over feature, the intensities of both CH_2 and CH_3 bands decreased, the band corresponding to the CH groups of Fc cp ring increases slightly. The most significant changes are found in the range between 2000-1000 cm^{-1}, where two new bands at 1751 cm^{-1} and 1474 cm^{-1} corresponding to C=O and C-N stretching modes appeared upon incubation with CB[7] (Figure 1B).[25] In addition, we have also observed a decrease in the water contact angles on the surface. As shown in the insets of Figure 1, the surface becomes more hydrophilic, which can be attributed to the surface-bound electronegative carbonyl portals of CB[7] (Scheme 1).

The above described structural characterization enabled us to confirm the binding of CB[7] on FcC11S-/C8S-Au; however, it is not feasible to provide further information regarding the formation thermodynamics/kinetics of Fc@CB[7] by either IR or wetting measurements. Due to their reversible redox responses, ferrocenylalkanethiolate SAMs on gold have been extensively studied with a range of electrochemical techniques for understanding interfacial electron transfer processes.[38-42] Herein we explore the feasibility of using conventional cyclic voltammetric (CV) measurements to probe the formation and stability of Fc@CB[7] at molecular interfaces. Figure 2 shows the CV responses of FcC11S-/C8S-Au before and after incubation with different concentrations of CB[7] ($c_{CB[7]}$). Consistent with our previous finding,[32] a single pair of symmetric peaks with $E^{\circ'}$ = + 262 mV (vs. Ag/AgCl) was observed for the initially prepared FcC11S-/C8S-Au. The peak width at the half-height (96.1 mV) is close to the theoretical value of 90.6 mV predicted from the Langmuir adsorption

isotherm.[35] Such a "near-ideal" redox behavior confirms that in FcC11S-/C8S-Au the Fc terminal groups are uniformly distributed and isolated from each other.[31,32] As shown in Figure 2, upon immersing with CB[7], the CV responses changed remarkably. As the concentration increases, it starts to show a shoulder peak at more positive potential which becomes dominate subsequently. The original peak not only becomes smaller, but also shifts positively upon increasing the concentration of CB[7]; in contrast the new peak only increases its intensity without significant potential shifts. Based on this observation, the CV peak at more positive potential should result from Fc@CB[7] formed on FcC11S-/C8S-Au. Such an assignment is also consistent with the fact the first peak eventually diminishes when the concentration of CB[7] reaches 80 μM, i.e., the Fc terminal groups on FcC11S-/C8S-Au are all bound with CB[7]. As depicted in Figure 2, the redox peaks corresponding to Fc^+/Fc and Fc^+@CB[7]/Fc@CB[7] are different not only in the formal potential (+ 262 mV and + 381 mV vs. Ag/AgCl), but also in the full width at the half-height (96 mV and 57 mV, respectively).

In accordance with previous studies of Fc@CB[7] host-guest binding in solution,[17,43] the positive formal potential shift may result from the fact that Fc^+ ions inside the hydrophobic inner cavity of CB[7] are less stable than in an aqueous environment. In our case, the surface tethered CB[7] may inhibit the ion-pairing between ClO_4^- ions in the electrolyte and Fc^+ encapsulated by CB[7], which also contributes to a positive potential shift.[34] Based on the theoretical *i-E* equation derived from Frumkin adsorption isotherm,[35,44] the narrowed CV peak can be attributed to the intermolecular attraction force among the adsorbed redox species, i.e., a so-called "outer-surface interaction" among Fc@CB[7] on surface.[45] The gradue shift of the formal potential for Fc/Fc^+ when increasing the concentration of CB[7] is another indication of "enhanced" intermolecular interactions on surface; the redox process of free Fc groups on the surface is also affected by the immobilized CB[7] neighbors, which eventually change their anionic microenvironment (the existence of electronegative carbonyl portals).

Because of the existence of intermolecular interactions among the surface tethered redox centers (Fc^+/Fc and Fc^+@CB[7]/Fc@CB[7]), the widely adopted Langmuir adsorption isotherm is not suitable for determining the binding constant (*K*) of CB[7] to FcC11S-/C8S-Au. Nevertheless, we can quantify the exact amount of both unbounded Fc and Fc@CB[7] from their corresponding CV peaks. As of the overlap between the two peaks (Figure 2), we have adopted the Gaussian-Lorentzian fitting protocol[33] to deconvolute them and to obtain the surface concentrations of Fc and Fc@CB[7] respectively, based on Eq. 1,[35]

$$\Gamma_{\mathrm{Fc}} = \frac{Q_{\mathrm{Fc}}}{nFA} \quad (1)$$

where Q_{Fc} is the integrated charge of Fc/Fc^{+} redox peak; n is the number of electrons involved in the redox reaction; F is the Faraday constant; A is the electrode area. The initial surface density of Fc (i.e., no CB[7] present in the solution) was determined to be $6.0\pm0.4 \times 10^{-11}$ mol/cm^2, which is lower than the theoretical surface density of a full CB[7] monolayer on gold (7.5×10^{-11} mol/cm^2).[20] This ensures that there are no spacial restrictions of CB[7] binding to FcC11S-/C8S-Au. In Figure 3(A), we have shown that with increased concentration of CB[7], the value of Γ_{Fc} decreases while that of $\Gamma_{\mathrm{Fc@CB[7]}}$ increases monotonically. At a high concentration of CB[7] ($\geq$ 80 μM), over 90 % of Fc groups are bound with CB[7]. With the above determined $\Gamma_{\mathrm{Fc@CB[7]}}$ and Γ_{Fc}, the calculation of K of Fc@CB[7] at the molecular interfaces is not difficult.

$$\mathrm{Fc@C11S\text{-}Au} + \mathrm{CB[7]} \rightleftharpoons \mathrm{CB[7]@FcC11S\text{-}Au} \quad (2)$$

$$K = \frac{\Gamma_{\mathrm{Fc@CB[7]}}}{\Gamma_{\mathrm{Fc}}\, c_{\mathrm{CB[7]}}} \quad (3)$$

As depicted in Figure 3(B), the K values showed no significant variations at different concentrations of CB[7] in the incubation solution. The average value ($7.3\pm1.8 \times10^{4}$ M^{-1}) indicates a moderate binding affinity between CB[7] and FcC11S-/C8S-Au SAMs, which is not as impressive as that determined in solution (3.2×10^{9} M^{-1}).[17] Unlike ferrocenemethanol in solution, the surface tethered Fc groups are lack of rotational freedom for taking the most energetically favored position inside CB[7], which may contribute to the decreased binding affinity. Moreover, the rather strong intermolecular interactions among Fc@CB[7] on FcC11S-/C8S-Au may also affect the hydrophobic interaction between CB[7] and the encapsulated Fc.[45] However, the K value determined here is much higher than previously reported Fc@CB[7] host-guest binding on surface tethdred CB[7] (3.4×10^{3} M^{-1})[24] or other host molecules (e.g., β-CD),[46] which confirms the improved stability of Fc@CB[7] formed at such an organized molecular interface.

In order to further understand the decreased formation constant of Fc@CB[7] at molecular interfaces with respect to homogenous solution phase, we proceed to investigate the binding and dissociation kinetics of CB[7] on FcC11S-/C8S-Au. The binding process was first studied by

measuring CV responses of FcC11S-/C8S-Au upon incubation in 1.0 mM CB[7] for different periods of time. Figure 4 shows that the peak corresponding to Fc^+/Fc diminishes rather rapidly, i.e., within 10 min the narrow peak corresponding to Fc^+@CB[7]/Fc@CB[7] becomes dominant. No further changes in the CV responses were observed when the incubation period reaches 90 min. As shown in Figure 5(A), the surface density of Fc^+/Fc decreases exponentially as a function of the incubation time. If we consider the binging process as an elementary process,[47-48] the rate law of CB[7] binding on FcC11S-/C8S-Au can be expressed as Eq. 4.

$$Rate = -\frac{d\Gamma_t}{dt} = k_1 c_{\mathrm{CB[7]}} \Gamma_{\mathrm{t}}(\mathrm{Fc}) \qquad (4)$$

Since the amount of CB[7] in the incubation solution is in large excess with respect to the surface concentration of Fc^+/Fc, the rate law can be simplified as Eq. 5,

$$Rate = -\frac{d(\Gamma_{\mathrm{t}})}{dt} = k'\Gamma_{\mathrm{t}}(\mathrm{Fc}) \text{ with } k' = k_1 c_{\mathrm{CB[7]}} \qquad (5)$$

where *k'* is the pseudo-first-order rate constant (apparent binding rate constant) at a certain concentration of CB[7]. The integration of Eq. 5 provides the direct correlation between the surface density of Fc^+/Fc and the reaction time,

$$\ln(\Gamma_{\mathrm{t}}/\Gamma_0)_{\mathrm{Fc}} = -k't + \mathrm{C} \qquad (6)$$

Figure 5(B) shows the expected linear relationship between $\ln(\Gamma_t/\Gamma_0)_{Fc}$ and reaction time (*t*), which validates the kinetic model described above. More importantly, we were able to determine the apparent binding rate constant (2.8±0.3 s^{-1}) from the slope of the best linear fit (Figure 5B). Based on Eq. 5 and the known concentration of CB[7] in solution, the binding rate constant of CB[7] on FcC11S-/C8S-Au were obtained (2.8±0.3 × 10^3 $M^{-1}s^{-1}$).

To investigate the dissociation process, i.e., the desorption of CB[7] from CB[7]@FcC11S-/C8S-Au, we have incubated FcC11S-/C8S-Au in 1.0 mM CB[7] solution for a prolonged period of time (> 3 h), then transferred it into a CB[7]-free electrolyte solution. As shown in Figure 6, the redox peaks corresponding to Fc@CB[7] gradually decreases, in the meantime a shoulder peak corresponding to Fc^+/Fc appeared at a more negative potential. Such a change becomes

less obvious with prolonged incubation, i.e., even after 5 h the Fc@CB[7] is still predominate, indicative of a rather slow disassociation kinetics. Simpler than the binding process, the dissociation of Fc@CB[7] can be directly treated as a first-order reaction, for which the rate laws are described as Eq. 7 and Eq. 8,

$$Rate = -\frac{d(\Gamma_t)}{dt} = k_{-1}\Gamma_t \text{ (Fc@CB[7])} \quad (7)$$

$$\ln(\Gamma_t/\Gamma_0)_{\text{Fc@CB[7]}} = -k_{-1}t + C' \quad (8)$$

where k_{-1} is the dissociation reaction rate constant of Fc@CB[7]. In Figure 7(A), we have shown the dependence of the surface concentration of Fc@CB[7] as a function of time, and the linearized results (according to Eq. 8) are displayed in Figure 7(B), which yields a k_{-1} of (0.08±0.01) s^{-1} for the dissociation of Fc@CB[7] at the monolayer surface. The kinetic fitting was limited to the early stage of the dissociation, which was less influenced by rather significant experimental uncertainties with prolonged incubation in CB[7]-free electrolyte (Figure 7A).

The impacts of the kinetic data obtained here are substantial; first is their correlation with the formation constant for the Fc@CB[7] inclusion complex determined above, the other is the comparison with the reaction kinetics in a homogenous solution. For the former, we can deduce the formation constant *K* based on the ratio of the binding rate constant (k_1) and dissociation rate constant (k_{-1}).[49] Thus obtained *K* value (3.5±0.8 × 10^4 M^{-1}) is somewhat smaller but at the same magnitude with the directly determined one (7.3±1.8 × 10^4 M^{-1}). A possible reason for this difference is the moderate solubility of CB[7] in aqueous solution,[14] which results in a faster dissociation of Fc@CB[7] in CB[7]-free electrolyte solution than in 1.0 mM CB[7]. Nevertheless, the consistency between the thermodynamic and kinetics results confirms our electrochemical approach as a convenient and reliable protocol for studying host-guest chemistry at redox-active molecular interfaces.

The comparison between these new kinetic parameters for the formation of Fc@CB[7] at molecular interfaces with those of solution-phase is more intriguing. We believe that the unique structure of CB[7] dictates its strong binding with Fc (Scheme 1A), which allows fast binding and slow dissociation processes in solution. The high binding affinity of CB[7] with small guest molecules (e.g., naphthylethylammonium cation, berberine, adamantyl) in aqueous solution has been attributed to their very large binding rate constant ($10^8 \sim 10^9$ $M^{-1}s^{-1}$)[47-48,50] which are close to the

diffusion-controlled process ($k_{diff} = 6.5\times10^9$ $M^{-1}s^{-1}$),[51] as well as their small dissociation rate constants ($10^{-1} \sim 10^3$ s^{-1}).[47-48] Compared with CB[7], CB[6] (with a smaller inner cavity) has a binding rate constant (< 10^4 $M^{-1}s^{-1}$) with guests (e.g., cycloalkylmethylamines, alkylammonium ions),[52-53] which is many orders of magnitude smaller; β-CD (with a similar sized inner cavity of CB[7] but unsymmetrical hydroxyl portals) has much higher dissociation rate constant ($10^5 \sim 10^7$ s^{-1}) with guests (e.g. naphthylethanols).[54]

Based on the large formation constant of ferrocenemethanol@CB[7] in solution (3.2×10^9 M^{-1})[17] and the high binding rate constant (i.e., close to diffusion-controlled process, ~ 10^9 $M^{-1}s^{-1}$), the estimated dissociation rate constant would be ~ 10^{-1} s^{-1}. This is very close to our experimentally determined value (0.08 s^{-1}), and that reported for the dissociation of neutral adamantyl (Ad) from self-assembled CB[7] monolayer on gold (0.03 s^{-1}).[50] It becomes evident that the major difference between the formation Fc@CB[7] at a molecular interface or a homogenous solution is the binding rate constants; the much smaller binding rate constant may be the overall effect of several factors. The carbonyl portals of surface-bound CB[7] molecules may generate an "enhanced" electronegative field that hinder the subsequent binding between CB[7] and FcC11S-/C8S-Au. In addition, the heterogeneity of the monolayer structure, e.g., partially folding of FcC11S-Au, may shelter Fc from binding with CB[7] in solution. The exact mechanism for the restricted binding between the host molecules with the guests at organized molecular interfaces certainly deserves further investigation from both experimental and theoretical perspectives, but is beyond the scope of this report.

4. CONCLUSION

It was confirmed experimentally that stable host-guest inclusion complex can be formed at organized molecular interfaces. As the first trial system, the formation of Fc@CB[7] at "near-ideal" redox self-assembled monolayers was evaluated based on our systematic electrochemical investigations. The thermodynamic study showed that Fc@CB[7] on FcC11S-/C8S-Au has a moderate formation constant, which is higher than those on physically deposited CB[7] monolayers. The kinetic results showed much lower binding rate constant but similar dissociation rate constant compared with those in solution. More importantly, the Fc-tethered redox SAMs provides a convenient platform not only for quantitatively investigating Fc@CB[7] host-guest binding at molecular interface, but also for immobilizing biomolecules for biosensor fabrication. Further investigations to improve the stability of Fc@CB[7] at molecular interfaces are currently underway in our laboratory.

Acknowledgements

We gratefully acknowledge the financial support from the Natural Sciences and Engineering Research Council (NSERC) of Canada (PI: H.Z.), the Natural Science Foundation of China (PI: H.S.), and China Scholarship Council (H.T. visiting fellowship).

Supporting Information

Details of the CV fitting data for obtaining the surface densities of Fc and Fc@CB[7] at varies experimental conditions. This information is available free of charge via the Internet at http://pubs.acs.org.

REFERENCE

(1) Lehn, J. M. Supramolecular chemistry: receptors, catalysts, and carriers. *Science* **1985**, *227*, 849-856.
(2) Beer, P. D.; Gale, P. A.; Smith, D. K. *Supramolecular chemistry*; Oxford University Press, 1999.
(3) Kaifer, A. E.; Li, W.; Yi, S. Cucurbiturils as versatile receptors for redox active substrates. *Isr*. *J*. *Chem*. **2011**, *51*, 496-505.
(4) Lee, J. W.; Samal, S.; Selvapalam, N.; Kim, H.-J.; Kim, K. Cucurbituril homologues and derivatives: new opportunities in supramolecular chemistry. *Acc*. *Chem*. *Res*. **2003**, *36*, 621-630.
(5) Lagona, J.; Mukhopadhyay, P.; Chakrabarti, S.; Isaacs, L. The cucurbit[n]uril family. *Angew*. *Chem*., *Int*. *Ed*. **2005**, *44*, 4844-4870.
(6) Masson, E.; Ling, X.; Joseph, R.; Kyeremeh-Mensah, L.; Lu, X. Cucurbituril chemistry: a tale of supramolecular success. *RSC Adv*. **2012**, *2*, 1213-1247.
(7) Isaacs, L. Cucurbit [n] urils: from mechanism to structure and function. *Chem*.*Commun*.**2009**, 619-629.
(8) Assaf, K. I.; Nau, W. M. Cucurbiturils: from synthesis to high-affinity binding and catalysis. *Chem*. *Soc*. *Rev*.**2015**, *44*, 394-418.
(9) Behrend, R.; Meyer, E.; Rusche, F. I. Ueber condensationsproducte aus glycoluril und formaldehyd. *Justus Liebigs Ann*. *Chem*. **1905**, *339*, 1-37.
(10) Kim, J.; Jung, I.-S.; Kim, S.-Y.; Lee, E.; Kang, J.-K.; Sakamoto, S.; Yamaguchi, K.; Kim, K. New cucurbituril homologues: syntheses, isolation, characterization, and X-ray crystal structures of cucurbit [n] uril (n= 5, 7, and 8). *J*. *Am*. *Chem*. *Soc*. **2000**, *122*, 540-541.
(11) Day, A.; Arnold, A. P.; Blanch, R. J.; Snushall, B. Controlling factors in the synthesis of cucurbituril and its homologues. *J*.*Org*.*Chem*. **2001**, *66*, 8094-8100.
(12) Freeman, W.; Mock, W.; Shih, N. Cucurbituril. *J*. *Am*.*Chem*. *Soc*.**1981**, *103*, 7367-7368.

(13) Biedermann, F.; Uzunova, V. D.; Scherman, O. A.; Nau, W. M.; De Simone, A. Release of high-energy water as an essential driving force for the high-affinity binding of cucurbit [n] urils. *J*. *Am*. *Chem*.*Soc*. **2012**, *134*, 15318-15323.
(14) Shetty, D.; Khedkar, J. K.; Park, K. M.; Kim, K. Can we beat the biotin–avidin pair?: cucurbit [7] uril-based ultrahigh affinity host–guest complexes and their applications. *Chem*. *Soc*. *Rev*. **2015**, *44*, 8747-8761.
(15) Cao, L.; Sekutor, M.; Zavalij, P. Y.; Mlinaric-Majerski, K.; Glaser, R.; Isaacs, L. Cucurbit [7] uril· guest pair with an attomolar dissociation constant. *Angew*. *Chem*. *Int*. *Ed*. **2014**, *53*, 988-993.
(16) Rekharsky, M. V.; Mori, T.; Yang, C.; Ko, Y. H.; Selvapalam, N.; Kim, H.; Sobransingh, D.; Kaifer, A. E.; Liu, S.; Isaacs, L. A synthetic host-guest system achieves avidin-biotin affinity by overcoming enthalpy–entropy compensation. *Proc*. *Natl*. *Acad*. *Sci*. **2007**, *104*, 20737-20742.
(17) Jeon, W. S.; Moon, K.; Park, S. H.; Chun, H.; Ko, Y. H.; Lee, J. Y.; Lee, E. S.; Samal, S.; Selvapalam, N.; Rekharsky, M. V. Complexation of ferrocene derivatives by the cucurbit [7] uril host: a comparative study of the cucurbituril and cyclodextrin host families. *J*. *Am*. *Chem*.*Soc*. **2005**, *127*, 12984-12989.
(18) Brinkmann, J.; Wasserberg, D.; Jonkheijm, P. Redox-active host-guest supramolecular assemblies of peptides and proteins at surfaces. *Eur*. *Polym*. *J*. **2016**, *83*, 380-389.
(19) Kim, K.; Selvapalam, N.; Ko, Y. H.; Park, K. M.; Kim, D.; Kim, J. Functionalized cucurbiturils and their applications. *Chem*. *Soc*. *Rev*. **2007**, *36*, 267-279.
(20) Lee, D.-W.; Park, K. M.; Gong, B.; Shetty, D.; Khedkar, J. K.; Baek, K.; Kim, J.; Rye, S. H.; Kim, K. A simple modular aptasensor platform utilizing cucurbit [7] uril and a ferrocene derivative as an ultrastable supramolecular linker. *Chem*. *Commun*. **2015**, *51*, 3098-3101.
(21) Tang, Y.; Yang, S.; Zhao, Y.; You, M.; Zhang, F.; He, P. The host–guest interaction between cucurbit [7] uril and ferrocenemonocarboxylic acid for electrochemically catalytic determination of glucose. *Electroanalysis* **2015**, *27*, 1387-1393.
(22) Neirynck, P.; Brinkmann, J.; An, Q.; van der Schaft, D. W.; Milroy, L.-G.; Jonkheijm, P.; Brunsveld, L. Supramolecular control of cell adhesion via ferrocene–cucurbit [7] uril host–guest binding on gold surfaces. *Chem*. *Commun*.**2013**, *49*, 3679-3681.
(23) Young, J. F.; Nguyen, H. D.; Yang, L.; Huskens, J.; Jonkheijm, P.; Brunsveld, L. Strong and reversible monovalent supramolecular protein immobilization. *ChemBioChem* **2010**, *11*, 180-183.
(24) Brinkmann, J. *Dynamic bioactive surfaces for cells using cucurbiturils*; University of Twente: Enschede, Netherlands, 2016.
(25) An, Q.; Li, G.; Tao, C.; Li, Y.; Wu, Y.; Zhang, W. A general and efficient method to form self-assembled cucurbit [n] uril monolayers on gold surfaces. *Chem*. *Commun*. **2008**, 1989-1991.
(26) Blanco, E.; Quintana, C.; Hernández, L.; Hernández, P. Atomic force microscopy study of new sensing platforms: cucurbit [n] uril (n= 6, 7) on gold. *Electroanalysis* **2013**, *25*, 263-268.
(27) Häkkinen, H. The gold-sulfur interface at the nanoscale. *Nat*. *Chem*. **2012**, *4*, 443-455.
(28) Love, J. C.; Estroff, L. A.; Kriebel, J. K.; Nuzzo, R. G.; Whitesides, G. M. Self-assembled monolayers of thiolates on metals as a form of nanotechnology. *Chem*. *Rev*. **2005**, *105*, 1103-1170.

(29) Vericat, C.; Vela, M. E.; Corthey, G.; Pensa, E.; Cortés, E.; Fonticelli, M. H.; Ibanez, F.; Benitez, G.; Carro, P.; Salvarezza, R. C. Self-assembled monolayers of thiolates on metals: a review article on sulfur-metal chemistry and surface structures. *RSC Adv*. **2014**, *4*, 27730-27754.
(30) Ulman, A. Formation and structure of self-assembled monolayers. *Chem*. *Rev*. **1996**, *96*, 1533-1554.
(31) Chidsey, C. E.; Bertozzi, C. R.; Putvinski, T.; Mujsce, A. Coadsorption of ferrocene-terminated and unsubstituted alkanethiols on gold: electroactive self-assembled monolayers. *J*. *Am*. *Chem*.*Soc*. **1990**, *112*, 4301-4306.
(32) Tian, H.; Xiang, D.; Shao, H.; Yu, H.-Z. Electrochemical identification of molecular heterogeneity in binary redox self-assembled monolayers on gold. *J*. *Phys*.*Chem*. *C* **2014**, *118*, 13733-13742.
(33) Lee, L. Y. S.; Sutherland, T. C.; Rucareanu, S.; Lennox, R. B. Ferrocenylalkylthiolates as a probe of heterogeneity in binary self-assembled monolayers on gold. *Langmuir* **2006**, *22*, 4438-4444.
(34) Rowe, G. K.; Creager, S. E. Redox and ion-pairing thermodynamics in self-assembled monolayers. *Langmuir* **1991**, *7*, 2307-2312.
(35) Bard, A. J.; Faulkner, L. R. *Electrochemical methods: fundamentals and applications*,*2nd edition*; John Wiley & Sons Inc.: Hoboken, U.S.A., **2001**.
(36) Popenoe, D. D.; Deinhammer, R. S.; Porter, M. D. Infrared spectroelectrochemical characterization of ferrocene-terminated alkanethiolate monolayers at gold. *Langmuir* **1992**, *8*, 2521-2530.
(37) Porter, M. D.; Bright, T. B.; Allara, D. L.; Chidsey, C. Structural characterization of n-alkyl thiol monolayers on gold by optical ellipsometry, infrared spectroscopy, and electrochemistry. *J*. *Am*. *Chem*.*Soc*. **1987**, *109*, 3559-3568.
(38) Smalley, J. F.; Finklea, H. O.; Chidsey, C. E.; Linford, M. R.; Creager, S. E.; Ferraris, J. P.; Chalfant, K.; Zawodzinsk, T.; Feldberg, S. W.; Newton, M. D. Heterogeneous electron-transfer kinetics for ruthenium and ferrocene redox moieties through alkanethiol monolayers on gold. *J*. *Am*. *Chem*.*Soc*. **2003**, *125*, 2004-2013.
(39) Weber, K.; Hockett, L.; Creager, S. Long-range electronic coupling between ferrocene and gold in alkanethiolate-based monolayers on electrodes. *J*. *Phys*.*Chem*. *B* **1997**, *101*, 8286-8291.
(40) Valincius, G.; Niaura, G.; Kazakevičienė, B.; Talaikytė, Z.; Kažemėkaitė, M.; Butkus, E.; Razumas, V. Anion effect on mediated electron transfer through ferrocene-terminated self-assembled monolayers. *Langmuir* **2004**, *20*, 6631-6638.
(41) Liu, B.; Bard, A. J.; Mirkin, M. V.; Creager, S. E. Electron transfer at self-assembled monolayers measured by scanning electrochemical microscopy. *J*. *Am*. *Chem*.*Soc*. **2004**, *126*, 1485-1492.
(42) Sumner, J.; Weber, K.; Hockett, L.; Creager, S. Long-range heterogeneous electron transfer between ferrocene and gold mediated by n-alkane and n-alkyl-carboxamide bridges. *J*. *Phys*.*Chem*. *B* **2000**, *104*, 7449-7454.
(43) Ong, W.; Kaifer, A. E. Unusual electrochemical properties of the inclusion complexes of ferrocenium and cobaltocenium with cucurbit [7] uril. *Organometallics* **2003**, *22*, 4181-4183.
(44) Laviron, E. Surface linear potential sweep voltammetry: Equation of the peaks for a reversible reaction when interactions between the adsorbed molecules are taken into account. *J*. *Electroanal*. *Chem*. **1974**, *52*, 395-402.

(45) Ni, X.-L.; Xiao, X.; Cong, H.; Zhu, Q.-J.; Xue, S.-F.; Tao, Z. Self-assemblies based on the "outer-surface interactions" of cucurbit [n] urils: new opportunities for supramolecular architectures and materials. *Acc*. *Chem*. *Res*. **2014**, *47*, 1386-1395.
(46) Rojas, M. T.; Koeniger, R.; Stoddart, J. F.; Kaifer, A. E. Supported monolayers containing preformed binding sites. Synthesis and interfacial binding properties of a thiolated. beta.-cyclodextrin derivative. *J*. *Am*. *Chem*.*Soc*. **1995**, *117*, 336-343.
(47) Tang, H.; Fuentealba, D.; Ko, Y. H.; Selvapalam, N.; Kim, K.; Bohne, C. Guest binding dynamics with cucurbit [7] uril in the presence of cations. *J*. *Am*. *Chem*.*Soc*. **2011**, *133*, 20623-20633.
(48) Miskolczy, Z.; Biczók, L. Kinetics and thermodynamics of berberine inclusion in cucurbit [7]uril. *J*. *Phys*.*Chem*. *B* **2014**, *118*, 2499-2505.
(49) Pauling, L. *General Chemistry*; Courier Corporation: North Chelmsford, U.S.A., **1988**.
(50) Alberto, G. C.; Pascal, J.; Jurriaan, H. Recognition properties of cucurbit[7]uril self-assembled monolayers studied with force spectroscopy. *Langmuir* **2011**, *27*, 11508-11513.
(51) Murov, S. L.; Carmichael, I.; Hug, G. L. *Handbook of photochemistry*; CRC Press: Boca Raton, U.S.A., **1993**.
(52) Marquez, C.; Nau, W. M. Two mechanisms of slow host–guest complexation between cucurbit [6] uril and cyclohexylmethylamine: pH−responsive supramolecular kinetics. *Angew*. *Chem*., *Int*. *Ed*. **2001**, *40*, 3155-3160.
(53) Mock, W. L.; Shih, N. Y. Dynamics of molecular recognition involving cucurbituril. *J*. *Am*. *Chem*.*Soc*. **1989**, *111*, 2697-2699.
(54) Barros, T.; Stefaniak, K.; Holzwarth, J.; Bohne, C. Complexation of Naphthylethanols with β-Cyclodextrin. *J*. *Phys*.*Chem*. *A* **1998**, *102*, 5639-5651.

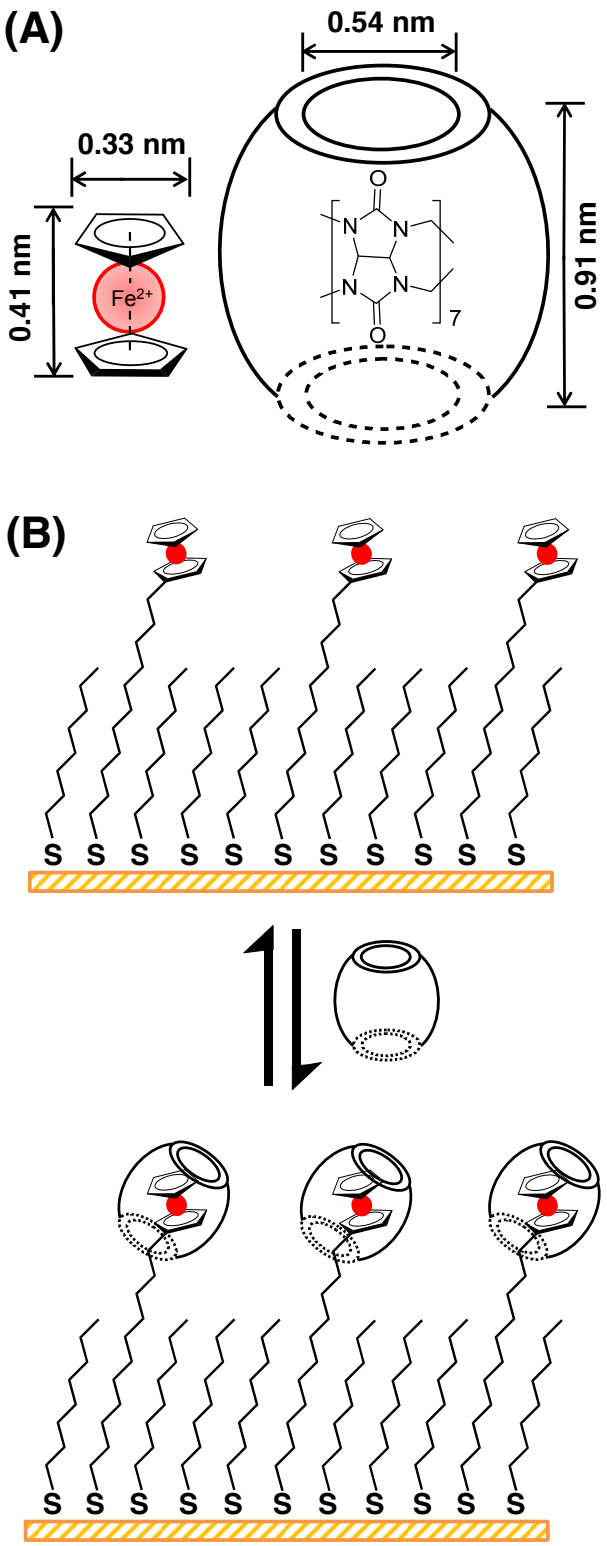

Scheme 1. (A) Illustration of the structure and size of ferrocene (Fc) and cucurbit[7] (CB[7]), respectively. (B) Host-guest binding between CB[7] and ferrocenylundecanthilate/octanethiolate SAMs on gold (FcC11S-/C8S-Au).

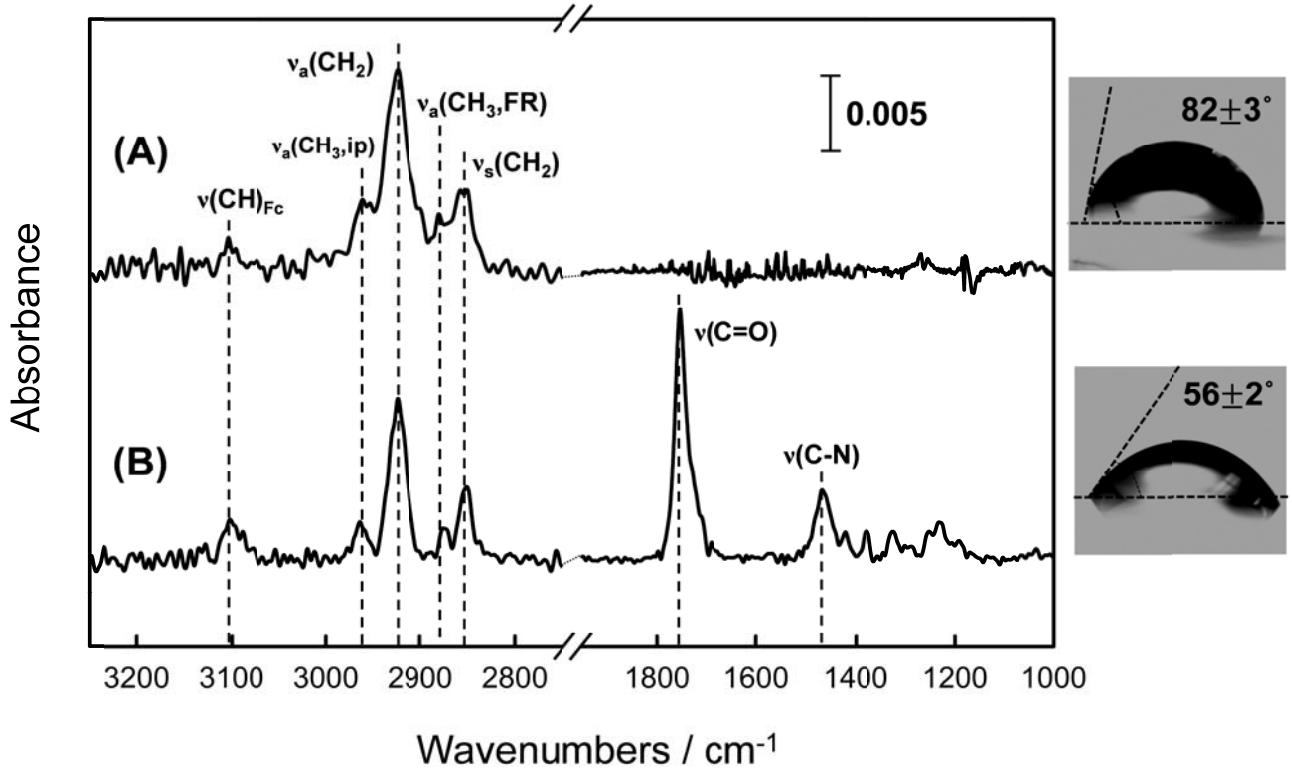

Figure 1. Reflection-adsorption FTIR spectra of FcC11S-/C8S-Au before (A) and after immersing in 1.0 mM CB[7] for 3 h (B). The right insets are the contact angles of water droplets on FcC11S-/C8S-Au before (top) and after immersing with CB[7] (bottom).

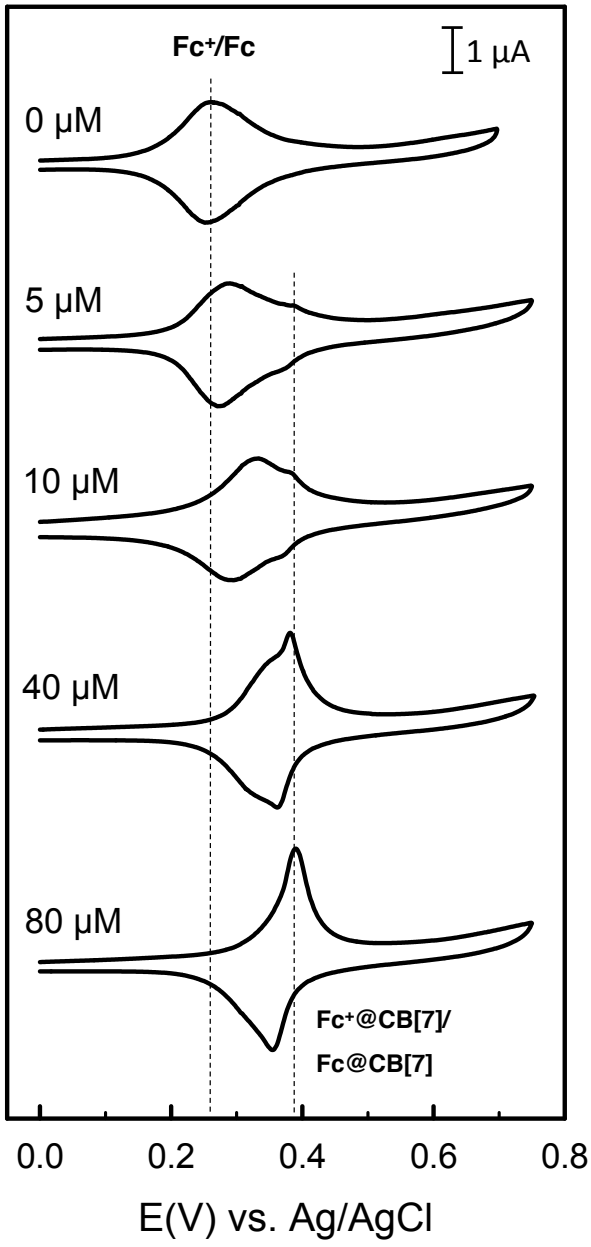

Figure 2. CVs of FcC11S-/C8S-Au before and after incubation with different concentrations of CB[7] for 3 h. The supporting electrolyte was 0.1 M $NaClO_4$, and the scan rate was 50 mV/s.

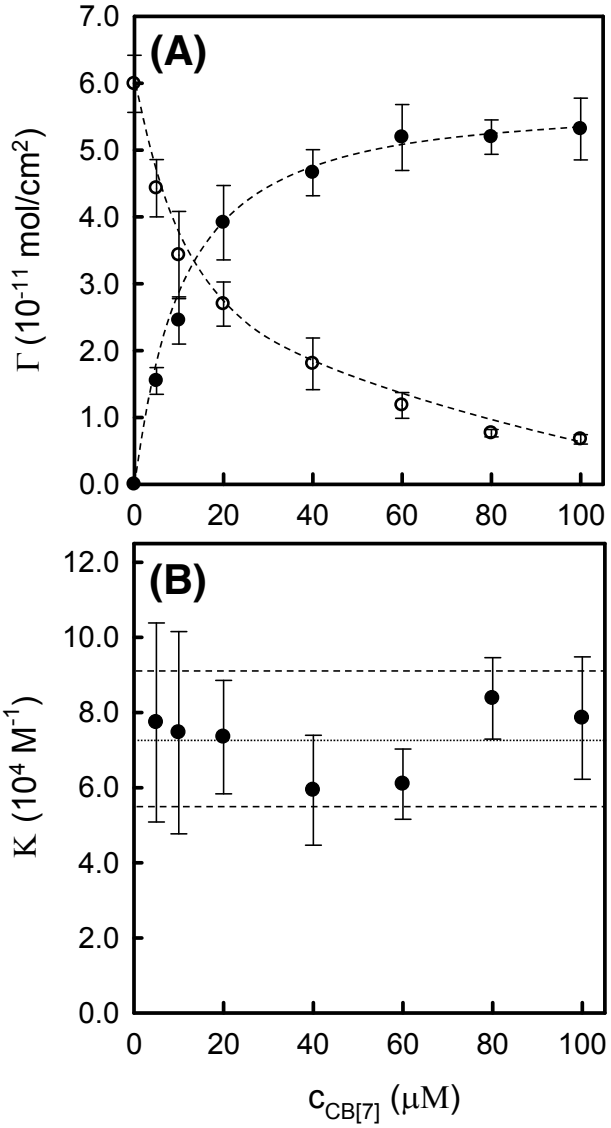

Figure 3. (A) Surface concentrations of Fc (open circles) and Fc@CB[7] (solid circles) on FcC11S-/C8S-Au upon reaching equilibrium with different concentrations of CB[7]. The dashed lines are to guide eyes only. (B) Formation constant (*K*) of Fc@CB[7] on FcC11S-/C8S-Au determined at different concentrations of CB[7] in solution. The dotted and dashed lines show the average and standard deviations of the determined *K*.

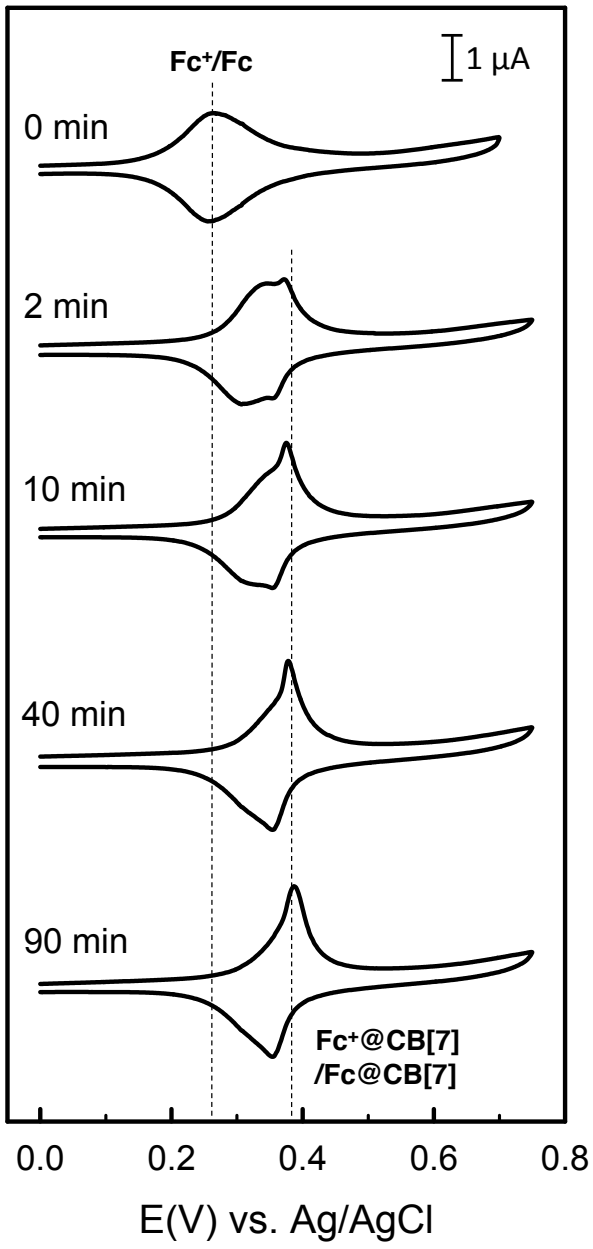

Figure 4. CVs of FcC11S-/C8S-Au before and after immersing with 1.0 mM CB[7] for different periods of time. The supporting electrolyte was 0.1 M $NaClO_4$, and the scan rate was 50 mV/s.

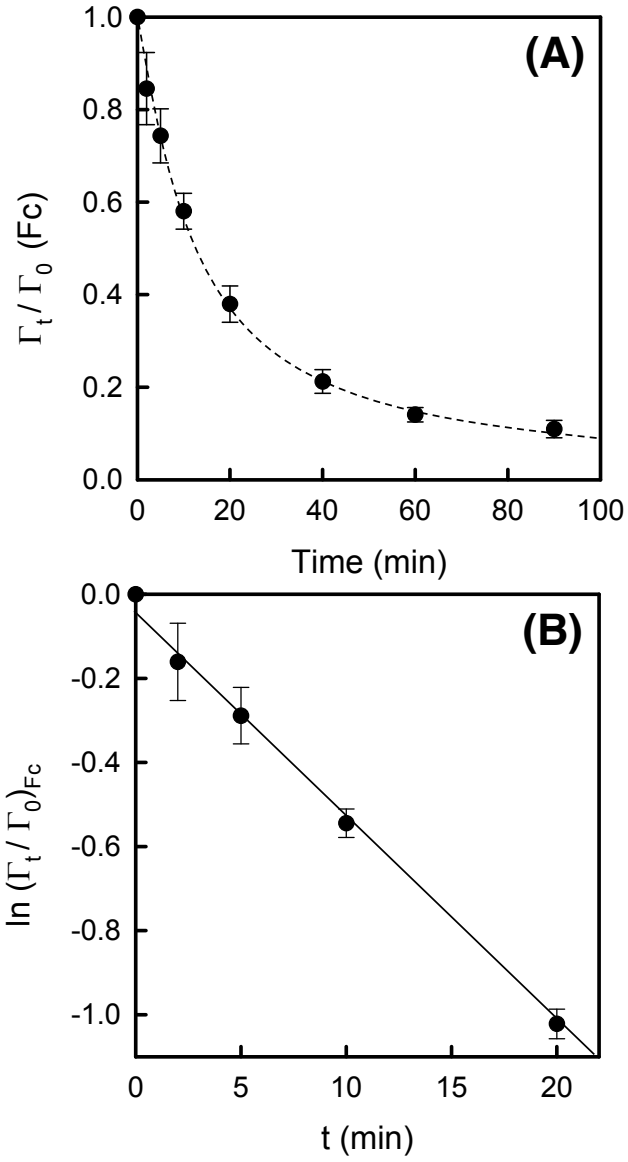

Figure 5. (A) Ratio between the surface concentration of Fc and its initial value (Γ_t/Γ_0) as a function of the immersing time in 1.0 mM CB[7] solution. The uncertainties were derived from three replicated experiments, and the dashed line is to guide eyes only. (B) The linear relationship between $\ln(\Gamma_t/\Gamma_0)_{Fc}$ and the CB[7] immersing time, from which the binding rate constant (k_1) of CB[7] on FcC11S-/C8S-Au was determined based on the pseudo-first-order kinetic model (see the text for details).

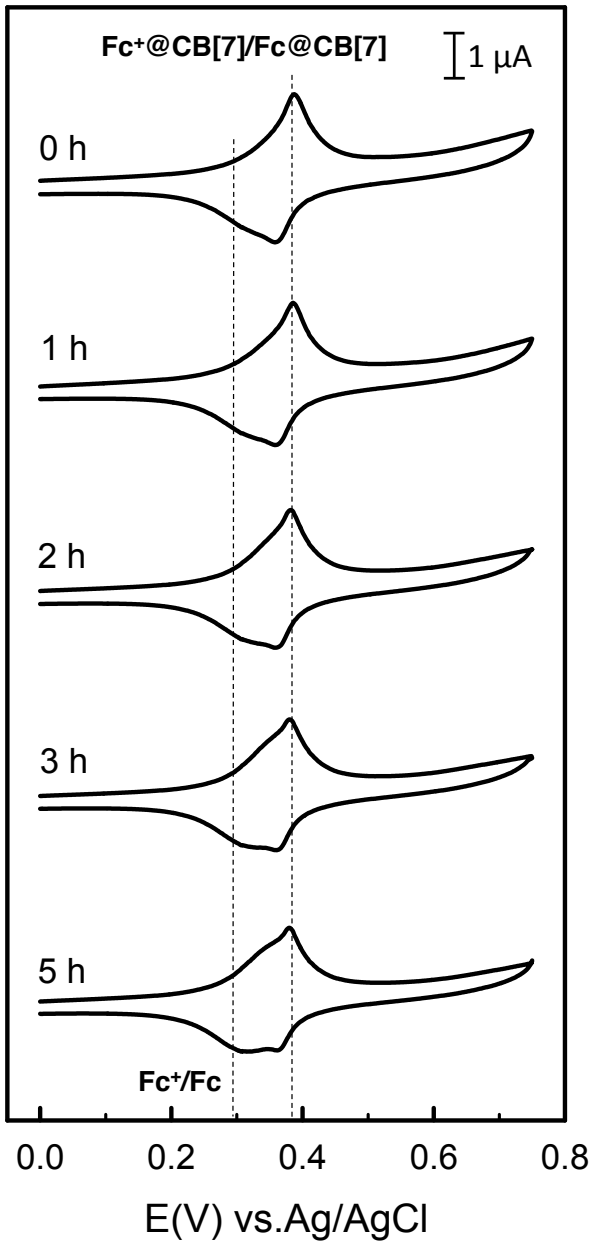

Figure 6. CVs of CB[7]@FcC11S-/C8S-Au initially prepared (upon incubation with 1.0 mM CB[7] for 3 h) and after immersing in CB[7]-free solution for different periods of time. The scan rate was 50 mV/s and the electrolyte was 0.1 M $NaClO_4$.

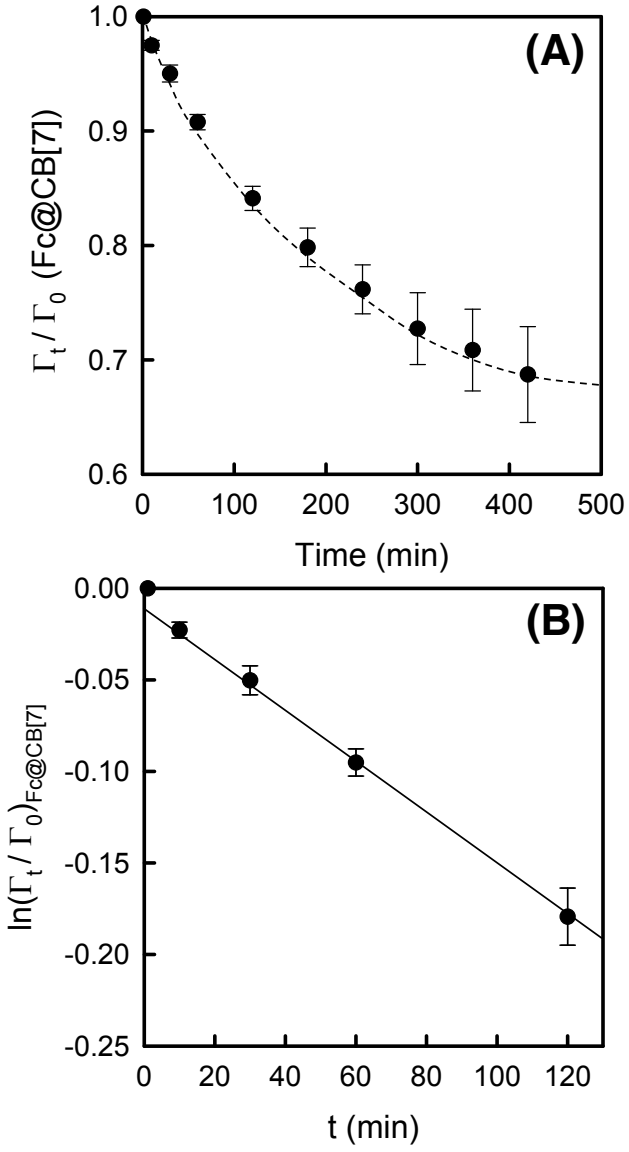

Figure 7. (A) Ratio between the surface concentration of Fc@CB[7] and its initial value (Γ_t/Γ_0) as a function of the incubation time in 0.1 M $NaClO_4$. The uncertainties were derived from three replicated experiments, and the dashed line is to guide eyes only. (B) The linear relationship between $\ln(\Gamma_t/\Gamma_0)_{Fc@CB[7]}$ and the incubation time, from which the dissociation rate constant (k_{-1}) of CB[7] from CB[7]@FcC11S-/C8S-Au was determined based on the first-order kinetic model (see text for details).

Toc graphic:

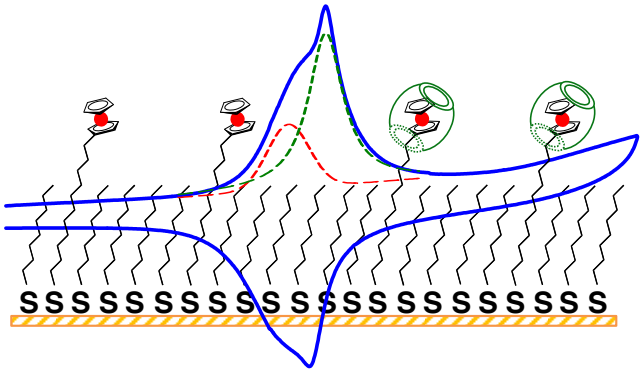

Supporting Information

For

Host-guest Interaction at Molecular Interfaces: Binding of Cucurbit[7]uril on Ferrocenyl Self-assembled Monolayers on Gold

Lin Qi,[†] Huihui Tian,[†,‡] Huibo Shao,[‡,*] and Hua-Zhong Yu[†,*]

[†]*Department of Chemistry, Simon Fraser University, Burnaby, British Columbia V5A 1S6, Canada*

[‡]*College of Chemistry and Chemical Engineering, Beijing Institute of Technology, Beijing 100085, China*
E-mail: hogan_yu@sfu.ca (H.Y.); hbs@bit.edu.cn (H.S.)

Deconvolution of the cyclic voltammograms (CVs) of FcC11S-/C8S-Au at various experimental conditions, from which the surface densities of Fc and Fc@CB[7] were determined (3 pages).

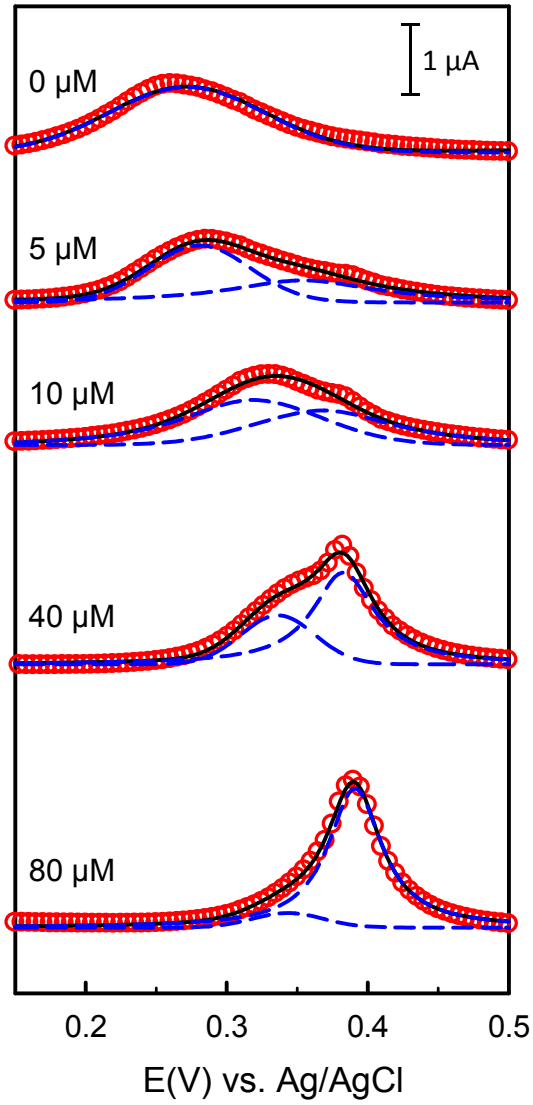

Figure S1 Gaussian-Lorentzian deconvolution of the CV anodic peaks of FcC11S-/C8S-Au before and after immersing with different concentrations of CB[7] for 3 h. The open circles (red) are the experimental data with the correction of the capacitive (baseline) current; the dashed lines in blue correspond to the deconvoluted peaks of Fc^{+}/Fc and Fc^{+}@CB[7]Fc@CB[7], respectively; the solid line in black is the sum of deconvoluted peaks (i.e., the overall fit).

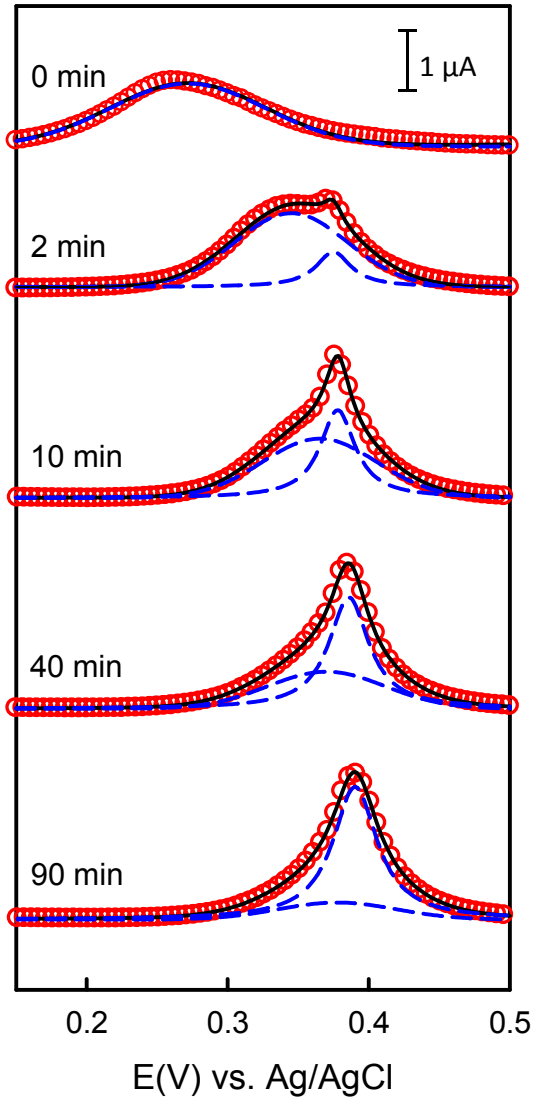

Figure S2 Gaussian-Lorentzian deconvolution of the CV anodic peaks of FcC11S-/C8S-Au before and after immersing with 1.0 mM CB[7] for different periods of time. The open circles (red) are the experimental data with the correction of the capacitive (baseline) current; the dashed lines in blue correspond to the deconvoluted peaks of Fc^{+}/Fc and Fc^{+}@CB[7]Fc@CB[7], respectively; the solid line in black is the sum of deconvoluted peaks (i.e., the overall fit to the experimental CV).

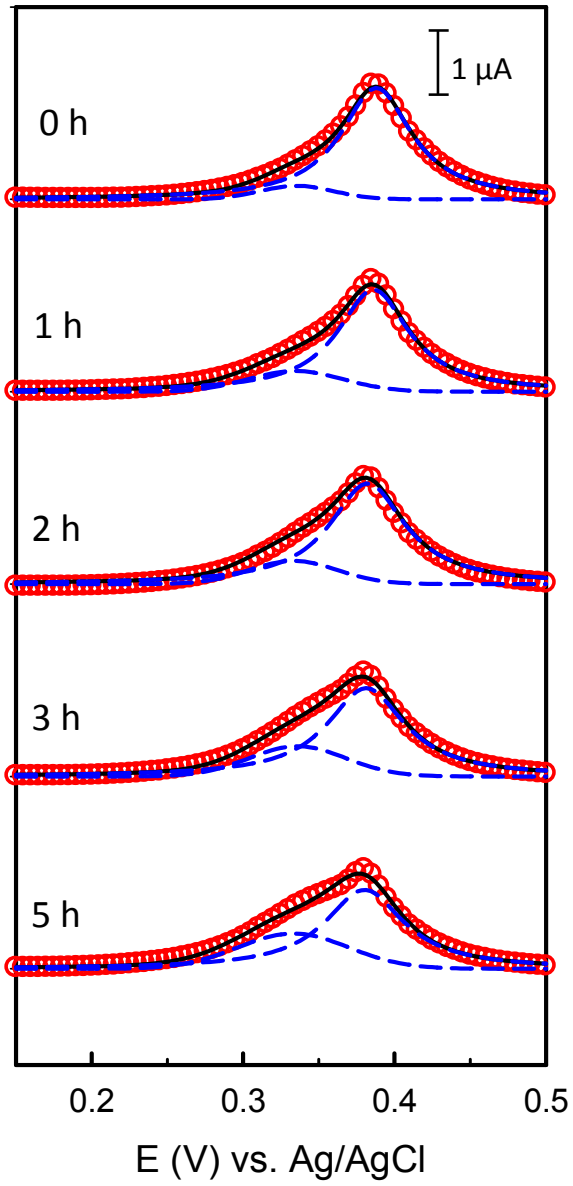

Figure S3 Gaussian-Lorentzian deconvolution of the CV anodic peaks of CB[7]@FcC11S-/C8S-Au before and after incubation in 0.1 M $NaClO_4$ for different periods of time. The open circles (red) are the experimental data with the correction of the capacitive (baseline) current; the dashed lines in blue correspond to the deconvoluted peaks of Fc^+/Fc and Fc^+@CB[7]Fc@CB[7], respectively; the solid line in black is the sum of deconvoluted peaks (i.e., the overall fit to the experimental CV).